

Large-Scale Magnetic Connectivity in CMEs

Yuzong Zhang^{1,2}, Jingxiu Wang^{1,3}, Gemma Attrill³
and Louise K. Harra^{3,1}

¹Solar Magnetism and Activity Group, NAOC, China; ²Department of Astronomy, Beijing Normal University, China; ³Mullard Space Science Laboratory, UCL, UK

Abstract. Five flare/CME events were selected in this study. One is on May 12, 1997, for which there is only two active regions on the visible solar disc, and the magnetic configuration is rather simple. For other cases, many active regions were visible. They are the flare/CME events that occurred on Bastille Day of 2000, Oct. 28, 2003, Nov. 7, 2004 and Jan. 20, 2005. By tracing the spread of EUV dimming, which was obtained by SOHO/EIT 195 Å fixed-difference images, we studied the CME initiation and development on the solar disc. At the same time we reconstructed the 3D magnetic structure of coronal magnetic fields, extrapolated from the observed photospheric magnetograms by SOHO/MDI. In scrutinizing the EUV brightening and dimming propagation from CME initiation sites to large areas with different magnetic connectivities, we determine the overall coupling and interacting of multiple flux systems in the CME processes. Several typical patterns of magnetic connectivity are described and discussed in the view of CME initiation mechanism or mechanisms.

Keywords. sun-magnetic field, sun-coronal mass ejection

1. Introduction

Coronal Mass Ejections (CMEs) are a type of large-scale solar activity. As observational signatures of CMEs on the visible solar disk, EUV (Extreme-ultraviolet) waves and dimmings attract particular attention. Coronal dimmings are a depletion of mass in the low corona. The distribution of coronal dimming can be obtained from fixed-difference ‘de-rotated’ images which show real changes relative to the selected reference frame before the event (Chertok and Grechnev, 2005).

Dimmings appear at the onsets of CMEs as large-scale regions of temporarily reduced brightness in EUV and soft X-ray emissions persisting for many hours (e.g., Thompson *et al.*, 1998; Webb, 2000). The coincidence of dimmings observed by different coronal lines supports the idea (Thompson *et al.*, 1998; Zarro *et al.*, 1999; Gopalswamy and Thompson, 2000; Harra and Sterling, 2001) that such dimmings are caused by the outflow of plasma for partial or complete opening of the magnetic field structures occurring in association with CMEs. There are two ways for the transport and release of energy in the corona by magnetic field, one is by a series of wave modes, the other is by changing the magnetic configuration through magnetic flux emergence and cancelation (Wang & Shi, 1993). Therefore, to understand and predict the CME initiation, the knowledge about the pre-CME magnetic configuration and connectivity is fundamental. Based on the boundary element method (BEM) (Yan and Sakurai, 2000; Wang *et al.*, 2002) we extrapolate the magnetic field from the photosphere into the corona. Our approach, then, is to correlate the EUV dimming regions, shown by EUV base difference images, with the topology skeleton revealed by the extrapolated magnetic lines of force.

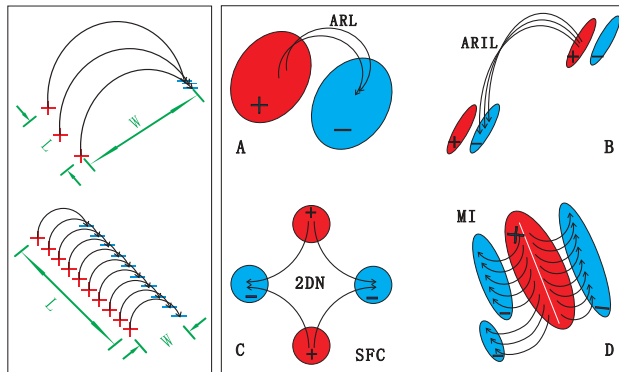


Figure 1. -Left: upper is cartoons of ‘loop’, lower, an ‘arcade’. ‘L’ denotes the length of footprints with same polarity, and ‘W’, the maximum width between positive and negative footprints. Right: magnetic connectivity and connecting patterns. ‘ARL’ is active region loop, ‘ARIL’, AR-interconnecting loop, ‘SFC’, saddle field configuration, ‘2DN’, 2- dimension null point, and ‘MI’,magnetic interface.

2. Data and Method

With heliograms of EIT aboard the Solar and Heliospheric Observatory (SOHO) in the coronal channel 195 Å of 12-minute cadence, we use the fixed-difference (or base-difference) de-rotated images to scrutinize the dimming development. Using the synoptic magnetic chart (Zhao and Hoeksema, 1997) as the boundary condition, we make the global potential extrapolation from solar photosphere to corona with BEM.

Form the properties of magnetic connectivity and footprints, we can classify field lines as magnetic ‘loop’ or magnetic ‘arcade’. As shown in the left of Figure 1, ‘L’ denotes the length of footprints with same polarity, and ‘W’, the maximum width between positive and negative footprints, if the value of L/W less than 2, we call this group of magnetic lines a ‘magnetic loop’ system; on the other hand, if it greater than or equal to 2, this group of lines, looks like an arch corridor, we call it a ‘magnetic arcade’ system. By the identical connectivity and similar curvature we divide extrapolated magnetic field lines into different loop systems. Firstly, based on the different types of connectivity, we define two types of loop systems, one is a simple inner loop of an active region or plage region, named as active region loop (ARL); the other type is the loops connecting opposite polarity flux from two different active regions or plage regions, named as AR-interconnecting loop (ARIL). Some ARILs are well-known transequatorial loops (TELs) which are often CME-associated (Khan & Hudson 2000). Sometimes, a few sets of magnetic loop systems are composed of several connecting patterns. Like the third case, each of four sets of magnetic loop systems connect two of the four coplanar magnetic poles. The magnetic lines of force, then, form a saddle field configuration (SFC). The configuration usually is large scale and contains TELs. As demonstrated by Wang and Wang (1996), there was a 2-dimensional null point in the center of the structure. Tsuneta (1996) provided evidence that transequatorial magnetic reconnection took place in this type of configuration from Yohkoh SXT images. In the fourth case, a few sets of magnetic lines of force root closely in the magnetic flux of the same AR or plage, then widely spread out from this set of footprints and connect broadly separated magnetic fields. They form a separatrix or quasi-separatrix layers (Priest & Démoulin 1995).

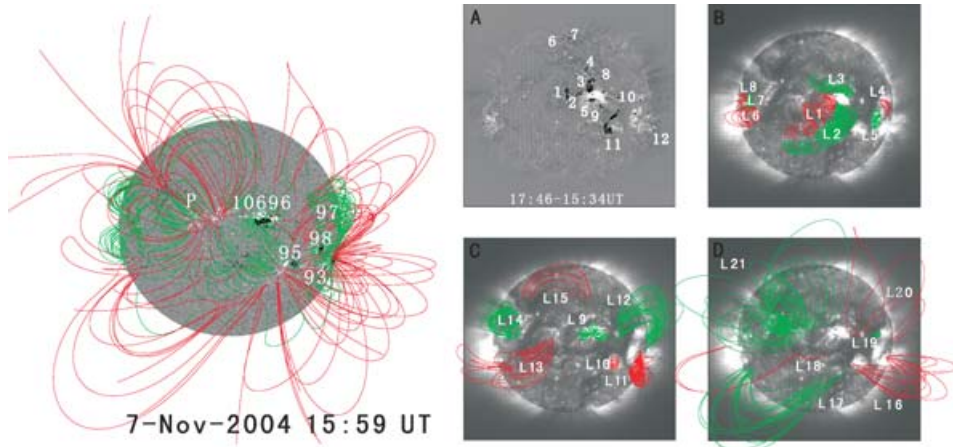


Figure 2. -Left: The 3-D extrapolated coronal magnetic field lines. Green lines with height ≤ 0.5 R_{sun}, red lines denoted >0.5 R_{sun} <2.5 R_{sun}, or open field lines. Right: Panel A is the fixed-difference image overlaid the contour of dimmings; Panel B-D are EIT image at 17:46 UT overlaid the magnetic loop systems.

3. The Event of 7 November 2004

On 7 November 2004 there was an X2.0 class flare at 15:42 UT, peaking at 16:06 UT and ending at 16:15 UT. At 16:54 UT, LASCO C2 detected a halo CME. Figure 2 (left) shows the extrapolated coronal magnetic field with the background of the MDI daily full disk magnetogram at 15:59 UT. Five active regions were on the visible solar disc. 'P' means a plage region. A transequatorial loop system connected AR 696 and AR 695. Two long arcades located at the region between AR 696 and AR 695 and there was a SFC under AR 696. There are 21 sets of magnetic different loop systems identified. At 18:20 UT, the dimming area reached its maximum and lasted for several hours. Dimmings appeared in a large range from East 10 degree to the west limb and from South 30 to North Pole (see Figure 2). It suggests that dimmings are large scale phenomenon and also suggests that plasma evacuation happened by the rapid expansion or 'opening' of the coronal magnetic field. Following the method of Attrill *et al.* (2006), we identify 12 dimming regions. Dimming regions, 2, 3, 5 and 9 linked to AR 696, and others were remote from AR 696. It is found that among these loop systems, L1, L2 and L3 are 'arcade' loop systems, others, 'loop' loop systems. Loop systems, L5, L7, L9, L10, L11 and L19 are ARLs, but others are IARLs.

We discover that for each dimming there is one or more loop systems involved (see Figure 2). Eleven of the total 21 loop systems are involved in the flare/CME event (see Table 1). It is also noticed that the upper half of the two arcade loops, 'L1' and 'L2', just locate on the four coplanar magnetic flux patches and form a SFC. In the center of SFC there is a 2-dimensional null point. Five dimming regions, 1, 2, 5, 9 and 11 developed from the 3 ends of the SFC. Under the arcade 'L2' an long dimming 'L9' developed along the right hand side footpoints.

4. Discussion and Conclusion

All of the events we studied have complicated magnetic topology on the visible solar disk. We also find key magnetic topology patterns, such as saddle field configuration and magnetic interface, which are associated with dimming (see Figure 3). Table 2 shows the number of loop systems involved in the dimming processes. For each major flare/CME

D	Connectivity	Property	D	Connectivity	Property
1	L1f L3f	ARIL(SFC) ARIL	7	L15b L21b	ARIL ARIL
2	L1f L3f L9f	ARIL(SFC) ARIL ARIL	8	L3b	ARIL
3	L3f L9f	ARIL ARL	9	L2b L9f	ARIL(SFC) ARL
4	L3f	ARIL	10	L12f L20b	ARIL ARIL
5	L1f L2f L9f	ARIL(SFC) ARIL(SFC) ARL	11	L2f L10f L12f L16f	ARIL ARL ARIL ARIL
6	L15b L21b	ARIL ARIL	12	L11b L16b	ARL ARIL

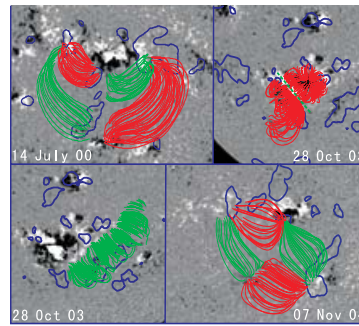


Table 1. ‘L’ means ‘Loop System’, ‘D’ means ‘Dimming’; ‘f’ means the dimming just on the foot of loop system, ‘b’ means the dimming on the beneath of the loop system. at 7 Nov.2004

Figure 3. shows magnetic connectivity patterns. The background are MDI magnetograms with contours of dimming regions.

Events	Total LSs	LSs in CME	P	Events	Total LSs	LSs in CME	P
Bastille Day	53	34	64	2004 November	21	11	52
Halloween Epoch	32	25	78	2005 January	17	11	65
1997 May	5	3	60				

Table 2. ‘LS’ means loop system; ‘P’ means percent.

event, more than 10 independent loop systems are involved in the processes leading to coronal dimming. This means that the source region of CMEs are an inter-coupling, multiple magnetic loop systems. It is of large scale in nature.

As a comparison, a quite simple flare/CME event on 12 May, 1997 is chosen. Only one active region is on disk center, the other on the west edge. Three of total five loop systems, i.e., 60 % of loop systems related to these dimmings.

Acknowledgements

Grateful to the SOHO/EIT team for the data used. Supported by National Key Basic Research Science Foundation of China (G2000078404), National Natural Science Foundation of China (10233050 and 10573025).

References

Attrill, G. D. R, *et al.* 2006, Solar Phys. (Submitted).
 Chertok, I.M. & Grechnev, V.V. 2005, Solar Phys. 229, 95.
 Gopalswamy N. & Thompson B.J. 2000, JASTP 62, 1427.
 Harra, L. K. and Sterling, A. C. 2001, ApJ, 561, L215.
 Khan, J.I. & Hudson, H.S. 2000, GRL 27, 1083.
 Priest, E. R., & Démoulin, P. 1995, J. Geophys. Res., 100, 23443.
 Thompson, B.J., Plunkett, S.P. and Gurman, J.B. 1998, GRL, 25, 2465.
 Tsuneta, S. 1996, ApJ, 456, L63.
 Wang, H.,& Wang, J. 1996, A&A, 313, 285.
 Wang, J., & Shi, Z. 1993, Solar Phys. 143, 119.
 Wang T., Yan Y. and Wang J. 2002, ApJ 572, 580.
 Webb, D. F., *et al.* 2000, J. Geophys. Res., 105, 27251.
 Yan Y. & Sakurai T. 2000, Solar Phys. 195, 89.
 Zarro, D.M., Sterling A.C. and Thompson B.J. 1999, ApJ 520, L139.
 Zhao, X., Hoeksema, J. T. and Scherrer, P. H. 1997, the Fifth SOHO Workshop, 751.